

1

2 Determinants of species-specific utilization of ACE2 3 by human and animal coronaviruses

4 Qingxing Wang¹, Sabrina Noettger¹, Qinya Xie¹, Chiara Pastorio¹, Alina Seidel¹,
5 Janis A. Müller^{1#}, Christoph Jung^{2,3,4}, Timo Jacob^{2,3,4}, Konstantin M.J. Sparrer¹, Fabian Zech¹,
6 and Frank Kirchhoff^{1*}

7

8 ¹Institute of Molecular Virology, Ulm University Medical Center, 89081 Ulm, Germany;

9 ²Institute of Electrochemistry, Ulm University, 89081 Ulm, Germany; ³Helmholtz-Institute Ulm
10 (HIU) Electrochemical Energy Storage, 89081 Ulm, Germany; ⁴Karlsruhe Institute of
11 Technology (KIT), 76021 Karlsruhe, Germany

12

13 # Current address: Institute of Virology, Philipps University Marburg, 35043 Marburg, Germany

14

15 * Address Correspondence to: Frank.Kirchhoff@uni-ulm.de

16

17 Running title: ACE2 usage by coronaviruses

18

19 **KEYWORDS:** SARS-CoV-2, bats, Spike glycoprotein, ACE2 receptor, zoonosis

20 **ABSTRACT**

21 Utilization of human ACE2 allowed several bat coronaviruses (CoVs), including the causative
22 agent of COVID-19, to infect humans either directly or via intermediate hosts. Here, we analyzed
23 the ability of Spike proteins from 24 human or animal CoVs to use ACE2 receptors across nine
24 reservoir, potential intermediate and human hosts. We show that overall SARS-CoV-2 Omicron
25 variants evolved more efficient ACE2 usage but mutation of R493Q in BA.5 Spike disrupts
26 utilization of ACE2 from Greater horseshoe bats. Spikes from most CoVs showed species-specific
27 differences in ACE2 usage, partly due to variations in ACE2 residues 31, 41 or 354. Mutation of
28 T403R allowed the RaTG13 bat CoV Spike to use all ACE2 orthologs analysed for viral entry.
29 Sera from COVID-19 vaccinated individuals neutralized the Spike proteins of a range of bat
30 Sarbecoviruses. Our results define determinants of ACE2 receptor usage of diverse CoVs and
31 suggest that COVID-19 vaccination may protect against future zoonoses of SARS-CoV-related
32 bat viruses.

33

34 **Highlights**

35 • Mutation of R493Q in BA.5 Spike disrupts utilization of ACE2 from Greater horseshoe bats
36 • Variations in ACE2 residues 31, 41 or 354 affect utilization by coronavirus Spike proteins
37 • Residue R403 in the Spike protein of bat coronavirus allow broad and effective ACE2 usage
38 • Sera from COVID-19 vaccinated individuals neutralize Spike proteins of bat Sarbecoviruses

39 **INTRODUCTION**

40 Coronaviruses (CoVs) have been detected in many animal species, including bats, swine, cattle,
41 horses, camels, cats, raccoon dogs, rodents, rabbits, ferrets, civets and pangolins^{1,2}. They are well
42 known to cross species barriers and have been successfully transmitted to humans at least seven
43 times³. Bats are the reservoir hosts and presumably all human CoVs (hCoVs) originate from bat
44 viruses, although transmission via intermediate hosts frequently facilitated viral zoonoses^{2,4}. Four
45 endemic human coronaviruses (hCoV-229E, -OC43, -NL63, -HKU1) have been circulating in the
46 human population for at least several decades and are responsible for a significant proportion of
47 seasonal common colds^{5,6}. While they are meanwhile well adapted to humans, it has been
48 suggested that they may have been more pathogenic early after transmission to humans⁷. Three
49 additional coronaviruses that emerged from viral zoonoses in the last 20 years cause severe disease.
50 SARS-CoV-1 was identified in 2003 as the causative agent of severe acute respiratory syndrome
51 (SARS), infected ~8.000 people, and was associated with a mortality of ~10%⁸. The Middle East
52 Respiratory Syndrome-CoV (MERS-CoV) emerged in 2012 with case fatality rates of almost
53 40%⁹. Only seven years later (December 2019), SARS-CoV-2, the causative agent of the COVID-
54 19 pandemic, was first detected^{10,11}. SARS-CoV-2 has a case fatality rate of less than 1% but
55 spread at an alarming rate and has caused over 700 million infections worldwide as of March 2023.
56 Both SARS-CoV-1 and SARS-CoV-2 belong to the *Sarbecovirus* subgenus of β -coronaviruses,
57 which are mainly found in bats¹² but have also been detected in pangolins and civets¹³⁻¹⁷.
58 Due to effective vaccines and increasing immunity, we are just gaining control over the SARS-
59 CoV-2 pandemic. However, at least seven independent zoonotic transmissions of animal
60 coronaviruses, including three highly pathogenic ones within the past 20 years, clearly highlight
61 that future zoonoses of bat CoVs pose a significant threat. The Spike (S) proteins of three of the
62 human coronaviruses, including SARS-CoV-1 and SARS-CoV-2, utilize the angiotensin-
63 converting enzyme 2 (ACE2) receptor for infection of human target cells¹⁸⁻²⁰. Thus, the ability of

64 CoVs to use human ACE2 for efficient entry plays a key role for successful zoonotic transmission.

65 Recently, a variety of bat CoVs that are related to human SARS- and MERS-CoVs have been

66 discovered and isolated^{21,22}. Alarmingly, a new study indicates frequent spillover of diverse bat

67 CoVs in human communities in contact with wildlife²³. Previous studies provided some insight

68 into the ability of Spike proteins from SARS-CoV-1, early SARS-CoV-2 variants, and the closely

69 related bat CoV RaTG13 to interact with different ACE2 orthologs^{13,24-29}. Altogether, however,

70 the ability of human, bat and other animal CoVs to utilize the ACE2 receptors of reservoir bats

71 species, putative intermediate hosts, and humans is poorly understood. Therefore, we analyzed the

72 ability of 24 Spike proteins from a variety of bat, civet, pangolin and human coronaviruses to use

73 ACE2 receptors from bat reservoir species, potential intermediate civet, pangolin, racoon dog,

74 camel, ferret and pig host, as well as humans. We found that single amino acid changes in Spike

75 proteins of human and bat CoVs can drastically change their ability to utilize ACE2 receptors

76 from these different species. Finally, we show that sera from individuals vaccinated against SARS-

77 CoV-2 neutralize infection mediated by Spike proteins from highly divergent bat CoVs.

78 **RESULTS**

79 **Expression of viral Spike proteins and ACE2 receptors from different species.** Bats are
80 considered the original reservoir hosts of all zoonotic coronaviruses. In several cases, however,
81 transmission to humans likely involved intermediate hosts, such as palm civets (SARS-CoV-1)¹⁷,
82 pangolins or raccoon dogs (SARS-CoV-2)^{15,16,30}, dromedary camels (MERS-CoV, hCoV-229E)³¹,
83 pigs (hCoV-OC43) or mice (hCoV-HKU-1) (**Figure 1a**). To better assess the risk of future
84 transmissions of coronaviruses to humans, we generated a collection of expression constructs of S
85 proteins from divergent bat CoVs, close relatives of SARS-CoV-1 and SARS-CoV-2 found in
86 civets and pangolins, respectively, as well as all seven hCoVs (Figure 1b, Table S1). To analyse
87 their function, we pseudotyped vesicular stomatitis virus (VSV) particles lacking the glycoprotein
88 (G) gene but encoding the green fluorescent reporter protein (VSVΔG-GFPpp) with these S
89 proteins. Western blot analyses showed that all S proteins were expressed at detectable albeit
90 variable levels in transfected HEK293T cells (Figure S1a). S-mediated entry depends on
91 proteolytic processing, e.g. by furin at the S1/S2 site, as well as TMPRSS2 or cathepsins^{32,33}. All
92 S proteins were processed and detected in the culture supernatants indicating incorporation into
93 VSVΔG-GFPpp (Figure S1a).

94 To determine species-dependent differences in the ability of ACE2 to mediate entry of human and
95 animal CoVs, we generated expression constructs for ACE2 orthologues from Greater horseshoe
96 bats (*Rhinolophus ferrumequinum*, *Rf*), Intermediate horseshoe bats (*Rhinolophus affinis*, *Ra*),
97 Sunda pangolin (*Manis javanica*), Masked palm civet (*Paguma larvata*), Common raccoon dog
98 (*Nyctereutes procyonoides*), Ferret (*Mustela putorius furo*), Camel (*Camelus dromedaries*), Pig
99 (*Sus scrofa domesticus*) and humans (**Figure 1c, Table S2**). ACE2 receptors from all species were
100 expressed at similar levels in transfected HEK293T cells (**Figure S1b**). This collection of
101 expression constructs allowed us to analyze the ability of S proteins from diverse animal and
102 human CoVs to utilize ACE2 from reservoir and intermediate hosts for viral entry.

103 **Species-specific ACE2 usage by SARS-CoV-2 variants.** Given the enormous spread of SARS-
104 CoV-2 it is a concern that emerging variants might establish reservoirs in animal hosts, such as
105 ferrets or pigs, mutate and be transmitted back to humans^{34–36}. To better assess this, we analyzed
106 the ability of different SARS-CoV-2 variants including Omicron variants of concern (VOCs) to
107 exploit ACE2 from various animal species. Infection assays using VSVΔG-GFPpp showed that S
108 proteins of the SARS-CoV-2 Hu-1, Delta and Omicron BA.1, BA.2 and BA.4/5 variants mediated
109 infection of HEK293T cells expressing ACE2 receptors derived from civet, pangolin, racoon dog,
110 camel, ferret, pig and intermediate horseshoe (*Ra*) bats (Figure 2a). Notably, infection via pig
111 ACE2 was generally most efficient. In comparison, the S proteins of the early Hu-1 variant and
112 the long-dominating BA.5 VOC (identical to BA.4) were unable to utilize ACE2 from greater
113 horseshoe bats (*Rf*) (Figure 2a). To challenge these findings and to assess the infection kinetics,
114 we used an approach allowing automated quantification of the number of VSVpp-infected (GFP+)
115 cells over time³⁷. The results confirmed that the BA.5 S usually shows increased infection
116 efficiencies compared to all remaining SARS-CoV-2 variants³⁸ but is unable to use *Rf* ACE2 for
117 infection (Figure S2). To further determine the fusogenic activity of SARS-CoV-2 S proteins in
118 cells expressing human or bat ACE2, we performed quantitative cell-cell fusion assays. All SARS-
119 CoV-2 S proteins promoted formation of large syncytia in cells expressing human or *Ra* ACE2
120 (S3). In agreement with the VSVpp infection data, however, the Hu-1 and BA.5 S proteins were
121 poorly active in mediating membrane fusion in cells expressing *Rf* ACE2. Thus, Omicron VOCs
122 evolved an increasing ability to use ACE2 orthologs of most species during adaptation to humans,
123 but the BA.5 variant lost the ability to use *Ra* ACE2 for entry.

124 **Residues R493 in Spike and D31/H41 in *Rf* ACE2 affect BA.5 entry.** The S protein of the
125 Omicron BA.5 variant differs only by deletion of amino acids 69 and 70 and changes of L452R,
126 F486V and R493Q from its BA.2 precursor³⁹. To determine which of these mutations is

127 responsible for the loss of *Rf* ACE2 usage, we introduced them individually into the BA.2 S
128 protein. All BA.2 mutant S proteins were efficiently expressed and processed (Figure 2b).
129 Mutation of R493Q disrupted the ability of the BA.2 S to use *Rf* ACE2 for viral entry (Figure 2c).
130 It has been reported that reversion of R493Q (Q493 is found in early SARS-CoV-2 strains,
131 including Hu-1) restores affinity for human ACE2 and consequently the infectiousness of
132 BA.4/5⁴⁰. Based on the modelled structure, R493 in S interacts with D31 and E35 in the *Rf* ACE2
133 and these interactions are disrupted by the R493Q substitution (Figure 2d). To further define S-
134 ACE2 interactions, we substituted nine amino acids of the *Rf* ACE2 by those found in *Ra* ACE2
135 (Figure S4). All mutant ACE2 proteins were expressed at similar levels but mutations of D31N
136 and H41Y as well as (to a lesser extent) K27I and N38D allowed them to mediate infection via the
137 BA.5 S protein (Figure 2e). Our results demonstrate that the R493Q change in CoV-2 S disrupts
138 utilization of ACE2 from *Rf* bats that are widespread in Europe, Northern Africa, and Asia. In
139 addition, we show that amino acid residues 31 and 41 play a role in the ability of ACE2 to serve
140 as receptor for CoV infection.

141 **Species-specific ACE2 usage by animal relatives of SARS-CoVs.** To determine the species-
142 specificity of ACE2 receptor usage by animal CoVs related to human SARS-CoVs, we
143 overexpressed human or animal-derived ACE2 in HEK293T cells and examined their
144 susceptibility to VSVpp infection mediated by S proteins from bat, pangolin, civet and human
145 CoVs. The collection encompassed S proteins of the closest relatives of SARS-CoV-1 and SARS-
146 CoV-2 detected in bats and potential intermediate civet and pangolin hosts, as well as some more
147 distantly related bat CoVs (Figure 1b). The early SARS-CoV-1 QXC2 strain used all ACE2
148 orthologs (except *Rf*), albeit generally with low efficiency (Figure 3a). In comparison, the closely
149 related TOR2 variant isolated in 2003 from a patient with SARS in Toronto⁴¹, showed about 3- to
150 4-fold higher infection rates indicating acquisition of increased ACE2 affinity during spread in

151 humans (Figure 3a). Surprisingly, VSVpp containing S proteins from closely related CoVs isolated
152 from civets (98.1% identity)⁴² and Rs3367 isolated in 2011 or 2012 from a Chinese Rufous
153 Horseshoe Bat (*Rhinolophus sinicus*) (91.9% identity)¹³ infected cells expressing all ACE2
154 receptors (except *Rf*) including the human ortholog with higher efficiency than those carrying
155 SARS-CoV-1 S (Figure 3a).

156 The S protein of BtKY72 obtained from Kenyan *Rhinolophus* bats⁴³ efficiently utilized the ACE2
157 receptors of *Rf* and *Ra* bats, as well as (unexpectedly) camel ACE2 and (to a lesser extent) palm
158 civet ACE2 for infection (Figure 3a). In contrast, the S protein of the related BM48 bat CoV⁴⁴
159 (Figure 1b) did not use ACE2 for entry. Sequence alignments show that all four ACE2 orthologs
160 allowing BtKY72 S-mediated infection contain mutations in an otherwise conserved lysin residue
161 K31N/D/E/T (Figure S5a). Amino acid 31 in ACE2 is in close proximity to the receptor binding
162 site (RBD) of S proteins (Figure S5b) and substitution of D31N in *Rf* ACE2 allowed it to serve as
163 entry receptor of BA.5 S (Figure 2e). Usage of *Ra* ACE2 for infection agrees with the previous
164 finding that it interacts with the RBD of the BtKY72 bat CoV²⁴. We found that *Rf* ACE2, which
165 can be used far less than *Ra* ACE2 as entry receptor, also allows efficient infection by the BtKY72
166 S (Figure 3a). The geographical distribution of *Ra* and *Rf* bats overlap and comprises North Africa
167 and large parts of Europe and Asia. Altogether, these results further support that residue 31 in
168 ACE2 plays an important role in S interation and suggest that some bat CoVs have the potential to
169 spread across three continents.

170 Spike proteins of the closest non-human relatives of SARS-CoV-2, RaTG13 sampled from a
171 *Rhinolophus affinis* horseshoe bat in 2013 in Mojiang, Yunnan (China) that shows 96.1% sequence
172 identity to SARS-CoV-2¹⁰, and CX-P1E obtained from tissue samples collected from Malayan
173 pangolins in 2017 and showing ~85.3% sequence identity¹⁵, used human ACE2 almost as
174 efficiently as the early Hu-1 CoV-2 strain (Figure 3a). However, both were more restricted than

175 Hu-1 S in the usage of ACE2 receptors from other species. For example, the wild-type RaTG13 S
176 allowed little if any infection of cells expressing pangolin, palm civet, ferret and *Rf* ACE2. We
177 have previously shown that a single change of T403 to R (found in the S proteins of most other *Ra*
178 bat CovS) in RaTG13 S strongly enhances infection via human ACE2²⁶. Thus, we examined
179 whether it has broader impact on ACE2 usage. Strikingly, utilization of all ACE2 orthologues was
180 increased by 3- to 57-fold and the mutant T403R RaTG13 S was capable of using all ACE2
181 orthologs at least as efficiently as the SARS-CoV-2 Hu-1 S for infection (Figure 3a). Sequence
182 analyses showed that E37 in ACE2 that is critical for the enhancing effect of the T403R mutation
183 is conserved in all but one ACE2 ortholog analyzed (Figure S6). The exception was the civet
184 ACE2, which contains a Q at this position and showed relatively poor efficiency in mediating
185 infection by the T403R RaTG13 S (Figure 3a).

186 The S proteins of bat CoVs that are more distantly related to SARS-CoV-2, i.e. Rc-0319, Rm1 and
187 *Rf*1 detected in *R. biasii*, *R. macrotis* and *Rf* bats, respectively (Figure 1b), were generally unable
188 to use any ACE2 ortholog for infection (Figure 3a). The only exception was that the Rc-0319 S
189 mediated infection via *Ra* ACE2, with significant albeit marginal efficiency (Figure 3a).
190 Automated quantification of the number of VSVpp-infected cells over time confirmed that the bat
191 Rs3367 and pangolin GX-P1E Spikes utilize all but the *Rf* ACE2 receptor with similar kinetics but
192 varying efficiencies (Figure 3b). The results also confirmed that T403R in RaTG13 S strongly
193 enhances infection by all nine ACE2 orthologs (Figure 3b). Finally, the infection kinetics verified
194 that the BtKY72 S uses camel, *Ra* and *Rf* ACE2 and (less efficiently) civet but not human,
195 pangolin, racoon dog, ferret or pig ACE2 for infection (Figure 3b). Although the BtKY72 S
196 efficiently utilized *Rf* and *Ra* ACE2 for infection of VSVpp (Figure 3a) it did not induce syncitia
197 formation in cell-to-cell fusion assays (Figure S7). Altogether, S proteins from bat CoVs show
198 striking and often species-specific differences in their ability to use ACE2 for infection, which are

199 in part determined by amino acid variations at position 403 in the viral S protein and 31 in the ACE2
200 receptors.

201 **G354 in ACE2 is critical for infection by hCoV-NL63.** Of the remaining five human CoVs only
202 the NL63 S is known to use human ACE2 for infection¹⁹. We addressed the possibility that S
203 proteins of hCoV-MERS, -229E, -OC43, -HKU1 or HKU9 from the related *Rousettus* bats may
204 use ACE2 orthologs from other species. In agreement with published data^{19,45}, however, only the
205 hCoV-NL63 S used ACE2 for infection (Figure 4a). While the hCoV-NL63 S mediated efficient
206 infection of cells expressing human, civet, raccoon dog, pig, camel or bat ACE2, it was unable to
207 utilize pangolin and ferret ACE2 (Figure 4a). Sequence analyses revealed that only the latter ACE2
208 orthologs contained substitutions (G354R and G354H) in an otherwise highly conserved glycine
209 residue (Figure 4b). The RBD of the hCoV-NL63 S has been well characterized^{25,45} and residue
210 G354 in ACE2 is directly involved in S-ACE2 interaction (Figure 4c). Molecular modeling of
211 S/ACE2 interaction using reactive force field simulations confirmed the establishment of close
212 proximity and putative interactions between the RBD of NL63 S and the ACE2 receptors. These
213 analyses predicted that substitutions of G354R and G354H weaken the interaction of ACE2 with
214 the NL63 S protein (Figure 4d). Altogether, these results indicate that hCoV-NL63 has the
215 potential to infect various animal species and suggest that G354 determines ACE2 usage by this
216 circulating hCoV.

217 **Sera from SARS-CoV-2 vaccinated individuals neutralize S proteins from bat CoVs.** In light
218 of previous coronaviral zoonoses, it is important to clarify whether vaccination against SARS-
219 CoV-2 may protect against future transmissions of bat CoVs to humans. To assess this, we
220 examined sera from ten individuals, five who received heterologous ChAdOx1 nCoV-
221 19/2xBNT162b2 and five who received 3xBNT162b2 prime-boost vaccinations^{46,47}. All sera
222 inhibited SARS-CoV-2 VOCs including Omicron BA.5, albeit the latter with reduced efficiency

223 (Figure 5a). It has been reported that sera obtained after SARS-CoV-2 vaccination neutralize S
224 proteins of SARS-CoV-1 and RaTG13^{26,48}. In agreement with this, infection mediated by S
225 proteins of the bat CoV Rs3367, which is closely related to SARS-CoV-1¹³, and the SARS-CoV-
226 2 related pangolin CoV Gx-P1E¹⁵, were inhibited as efficiently as SARS-CoV-2 variants (Figure
227 5a, Figure S8). To test neutralization under particularly challenging conditions, we examined the
228 effects on infection mediated by the BtKY72 S that shows only ~72% amino acid identity to the
229 SARS-CoV-2 Spike. As outlined above, BtKY72 does not use human ACE2 for infection (Figure
230 3a). Thus, *Rf* and *Ra* ACE2 were used in these experiments. Despite limited homology to the
231 SARS-CoV-2 S and utilization of bat ACE2, BtKY72 S-mediated viral entry was efficiently
232 neutralized by sera from COVID-19 vaccinated individuals (Figure 5a, Figure S8). In comparison,
233 only marginal effects were observed on infection mediated by the MERS-CoV S protein that shows
234 only 34.8% amino acid identity to the SARS-CoV-2 S.

235 The efficiency of neutralization varied between donors in both the AZ2xBNT and 3xBNT groups
236 (Figure 5b). On average, however, the IC₅₀ values of sera from both groups against the different S
237 protein correlated very well (Figure 5c). Predictably, the BA.5 S was less sensitive to neutralization
238 than Hu-1, with the remaining CoV-2 S proteins showing intermediate phenotypes. Sensitivities
239 of S proteins from bat CoVs to neutralization were within the same range and correlated with their
240 homology to the SARS-CoV-2 S, with RaTG13 being the most and BtKY72 being the least
241 sensitive (Figure 5c). In addition, the strength of ACE2 usage had an impact since neutralization
242 of RaTG13 T403R S required higher doses compared to the parental S protein. Similarly, BtKY72
243 S-mediated entry via *Ra* ACE2 was more efficient than via *Rf* ACE2 (Figure 3a) and the average
244 IC₅₀ for neutralization was 2- to 3-fold increased (Figure 5c). Altogether, these results strongly
245 suggest that prime-boost vaccination against SARS-CoV-2 will protect against future zoonoses of
246 bat *Sarbaocoviruses*.

247 **DISCUSSION**

248 The ability of CoVs to cross species barriers and the importance of utilization of the human ACE2
249 receptor for successful transmission to humans is established. However, the spectrum of ACE2
250 receptor usage by animal CoVs that may cause future zoonoses and the mechanisms underlying
251 species-specific differences are poorly understood. Here, we analyzed the ability of S proteins
252 from all seven human CoVs, as well as related CoVs from reservoir bat or potential intermediate
253 animal hosts, to use the ACE2 orthologs from nine different species for viral entry. We found that
254 CoV S proteins differ in their ability to utilize ACE2 for infection from efficient usage of all
255 orthologs, over species-specific to complete lack of utilization (Figure 6a). In addition, we provide
256 evidence that changes of R493Q in SARS-CoV-2 and T403R in RaTG13 bat CoV S proteins, as
257 well as D31N, H41Y or G354R/H in ACE2 receptors, play key roles in the species-specificity and
258 efficiency of ACE2 receptor usage by human and animal CoVs. Altogether, our data suggest that
259 ACE2 usage may allow human and animal CoVs to spread between all nine species examined
260 (Figure 6b). Encouragingly, however, our results further show that sera from individuals
261 vaccinated against SARS-CoV-2 neutralize infection mediated by S proteins from divergent bat
262 CoVs via both human or bat ACE2 receptors.

263 Mutation of R493Q distinguished BA.4/5 from BA.2. This change represents a reversion to early
264 SARS-CoV-2 strains and enhances S affinity for the human ACE2 receptor and consequently the
265 replicative fitness of BA.4/5 in human cells⁴⁹. Thus, it came as a surprise that mutation of R493Q
266 specifically disrupted the ability of the Omicron BA.2 S protein to use *Rf* ACE2 for infection.
267 These results show that viral adaption for efficient utilization of human ACE2 may come at the
268 cost of loosing the ability to utilize the ACE2 receptor from another species. Notably, the early
269 Hu-1 variant also contains 493Q and is unable to utilize *Rf* ACE2 (Figure 2). Thus, we identified
270 an example of expanded ACE2 tropism from Hu-1 to BA.1 and BA.2 that was lost again in BA.4/5.
271 Published data suggest that Q493R initially emerged because it mediates antibody resistance and

272 then reverted to regain efficient receptor binding when additional mutations allowed extended
273 antibody evasion⁴⁹. Notably, the effect of the R493Q mutation on ACE2 usage was highly specific
274 since this substitution exclusively impaired the interaction with *Rf* ACE2 and none of the other
275 ACE2 orthologs, including that from *Ra* bats.

276 We have previously shown that an amino acid change of T403R allows the S protein of RaTG13,
277 one of the closest bat relatives of SARS-CoV-2¹⁰, to efficiently utilize human ACE2 for viral
278 entry²⁶. Here, we demonstrate that the T403R change boosts utilization of ACE2 receptors from
279 all species analyzed. In several cases, infection mediated by the parental RaTG13 S was close to
280 background levels but became as least as efficient as infection mediated by SARS-CoV-2 S upon
281 introduction of the T403R mutation (Figure 3). Notably, the 3- to ~50-fold enhancement of
282 infection by the various ACE2 orthologs in transient transfection assays most likely underestimates
283 the effects of the T403R substitution under more physiological settings. In fact, the enhancing
284 effect of T403R on RaTG13 S-mediated infection of human lung cells or hPSC-derived gut
285 organoids was substantially higher for endogenous ACE2 than in cells overexpressing human
286 ACE2²⁶. Our results substantiate the key role of 403R that is found in the S proteins of most bat
287 CoVs in efficient utilization of ACE2 from different species.

288 While T403R RaTG13 S was able to utilize ACE2 from all nine species analyzed, the BtKY72
289 and Rc-0319 S proteins showed more limited and specific ACE2 usage. As an extreme, the Rc-
290 0319 S only mediated infection via *Ra* ACE2 and only with low efficiency (Figure 3a). In
291 comparison, the BtKY72 S used *Rf*, *Ra* and camel ACE2 with high and palm civet ACE2 with
292 moderate efficiency but none of the other five ACE2 orthologs. Our results indicate that mutations
293 of K31N/D/E/T allow utilization of ACE2 orthologs for BtKY72 S-mediated infection. Notably,
294 the geographic distributions and habitats of *Ra* and *Rf* bats overlap⁵⁰. *Ra* is found in many countries
295 in Southeast Asia, while *Rf* is distributed throughout Europe, Asia, and parts of Africa. CoVs
296 closely related to SARS-CoV-2 have been identified in *Ra* bats in China and this bat species is one

297 of the possible reservoir hosts for the origin of the COVID-19 pandemic. Another virus (RmYN02)
298 that is related to SARS-CoV-2 has been identified in *Rhinolophus ferrumequinum* bats in Japan⁵¹.
299 Our finding that some bat CoVs use the ACE2 receptors from both bat species suggests that SARS-
300 CoV-related viruses may have the potential to spread throughout large parts of Europe, Asia, and
301 parts of Africa by jumping from *Ra* to *Rf* bats. This agrees with the recent identification of SARS-
302 CoV-related Sarbecoviruses in European horseshoe bats in Europe⁵².
303 The circulating hCoV-NL63 is also thought to have originated in bats, and closely related CoVs
304 have been detected in *Pipistrellus* and *Rhinolophus* bats^{6,53}. We found that the hCoV-NL63 S
305 efficiently utilizes bat and human, as well as camel, pig, palm civet and raccoon dog ACE2 for
306 infection. Thus, this common cold virus that has been discovered almost 20 years ago⁵⁴ should
307 have the potential to infect various animal species. However, to our knowledge, no human-to-
308 animal transmissions have been documented. In contrast, the NL63 S was unable to use pangolin
309 and ferret ACE2 for infection. Lack of function is most likely due to species-specific changes of
310 G354H/R in the ACE2 interaction site with the receptor-binding domain (RBD) of the hCoV-
311 NL63 protein (Figure 4). Thus, a single amino acid change in ACE2 may disrupt utilization by the
312 S protein of a circulating hCoV and residue G354 seems to play an important role in the species-
313 specificity of S-ACE2 interaction.
314 One important question is whether COVID-19 vaccination may provide protection against future
315 zoonotic coronaviruses. In support of this, we have previously shown that the T403R RaTG13 S
316 is sensitive to sera from vaccinated individuals²⁶. This was expected since RaTG13 and SARS-
317 CoV-2 Spike show ~97.5% identity and sera from vaccinated individuals also neutralize the
318 SARS-CoV-1 S that shows only 76% homology to that of SARS-CoV-2^{55,56}. Here, we expanded
319 these analyses to more divergent bat CoVs. We found that sera from vaccinated individuals even
320 prevent infection mediated by the BtKY73 S, which shows ~72.0% identity to the SARS-CoV-2
321 S, via bat ACE2 receptors (Figure 5c). On average, S proteins from SARS-CoV-2 variants and

322 different bat CoVs showed similar sensitivities to neutralization, although BA.5 S shows just
323 ~2.7% and the BTKY73 S ~28.0% sequence divergence from the Spike proteins used for
324 vaccination. This illustrates that many changes evolving in SARS-CoV-2 Omicron VOCs become
325 fixed because they allow evasion of humoral immune responses.

326 In conclusion, our results show that ACE2 usage by S proteins of human and animal CoVs is often
327 broad. However, single amino acid changes in both S and ACE2 can drastically change the
328 efficiency of S-mediated virus infection via ACE2 orthologs from specific species. In addition, we
329 show that increased utilization of human ACE2 may come at the cost of losing the ability to use
330 ACE2 from a bat species. Our results further suggest that bat CoVs closely related to SARS-CoVs
331 have the potential to spread between different species of *Rhinolophus* bat that altogether are widely
332 distributed across Asia, Africa and Europe. On a positive note, vaccination against SARS-CoV-2
333 might confer efficient protection against future zoonoses of bat sarbecoviruses.

334 **Methods**

335 **Materials & Correspondence**

336 Further information and requests for resources and reagents should be directed to and will be
337 fulfilled by Frank Kirchhoff (frank.kirchhoff@uni-ulm.de).

338 **Cell culture.** All cells were cultured at 37 °C in a 5% CO₂ atmosphere. Human embryonic kidney
339 293T cells purchased from American type culture collection (ATCC: #CRL3216) were cultivated
340 in Dulbecco's Modified Eagle Medium (DMEM, Gibco) supplemented with 10% (v/v) heat-
341 inactivated fetal bovine serum (FBS, Gibco), 2 mM L-glutamine (PANBiotech), 100 µg/ml
342 streptomycin (PANBiotech) and 100 U/ml penicillin (PANBiotech). Mouse I1-Hybridoma cells
343 (ATCC:#CRL2700) were cultured in Roswell Park Memorial Institute (RPMI) 1640 medium
344 supplemented with 10% (v/v) heat-inactivated fetal bovine serum, 2 mM L-glutamine, 100 mg/ml
345 streptomycin and 100U/ml penicillin.

346 **Pseudoparticle production.** To produce pseudotyped VSVΔG-GFP particles, 6x10⁶ HEK 293T
347 cells were seeded 18 h before transfection in 10 cm dishes. The cells were transfected with 15 µg
348 of a glycoprotein expressing vector using TransIT®-LT1 (Mirus). 24 h post-transfection, the cells
349 were infected with VSVΔG-GFP particles pseudotyped with VSV G at an MOI of 3. One h post-
350 infection, the inoculum was removed. VSVΔG-GFP particles were harvested 24 h post-infection.
351 Cell debris was pelleted and removed by centrifugation (500 × g, 4°C, 5 min). Residual input
352 particles carrying VSV-G were blocked by adding 10% (v/v) of I1 Hybridoma Supernatant (I1,
353 mouse hybridoma supernatant from CRL-2700; ATCC) to the cell culture supernatant.

354 **Structure modeling.** The structure complex of SARS-CoV-2 BA.2 spike with or without R493Q
355 and *R. ferrumequinum* ACE2 was homology modeled using SWISS-MODEL
356 (<https://swissmodel.expasy.org/>), based on the structure of SARS-CoV-2 BA.2 spike complexed
357 with mouse ACE2 (mACE2) (PDB codes 8DM7)⁵⁷. The structure complexes of BtKY72 RBD and

358 *R. Affinis* ACE2 with WT/N31D/N31K were homology modeled using SWISS-MODEL
359 (<https://swissmodel.expasy.org/>), based on the structure of SARS-CoV-2 Hu.1 spike complexed
360 with *R. Affinis* ACE2 (*RaACE2*) (PDB codes 7XA7)⁵⁸. Molecular graphics visualization and
361 analyses were performed using the UCSF Chimera software (<http://www.rbvi.ucsf.edu/chimera>).

362 **Expression constructs.** pCG plasmids coding SARS-CoV-2 Spike Wuhan-hu-1 (NCBI reference
363 Sequence YP_009724390.1), Delta, BA.1, BA.2, or BA.5 were kindly provided by Stefan
364 Pöhlmann (Göttingen, Germany). Spike genes are listed in supplemental Table 1 and were
365 synthesized by Twist Bioscience, PCR amplified and subcloned into a pCG-strep expression
366 construct using the In-Fusion® HD Cloning Kit (Takara) according to the manufacturer's
367 instructions. pTwist EF1 Alpha-V5 tag plasmids expressing different ACE2 orthologs
368 (supplemental Table 2) were also synthesized by Twist Bioscience. pTwist EF1 Alpha-V5 tag
369 vector, pCG-strep vector, pCG-BatCoV-RaTG13 spike T403R, and pTwist EF1 Alpha-
370 Rhinolophus ferrumequinum ACE2 with mutations of L24R, K27I, D31N, S34H, N38D, H41Y,
371 F83Y S849, or S387T were generated using the In-Fusion® HD Cloning Kit (Takara). SARS-
372 CoV-2 Spike BA.2 spike with mutations of Δ69-70, L452R, F486V, or R493Q were generated
373 using Q5 Site-Directed Mutagenesis Kit (NEB). All constructs were verified by Sanger sequencing
374 in Microsynth seqlab. Primer sequences are listed in Supplementary table S1.

375 **GFP-Split fusion assay.** To detect formation of syncytia, HEK293T cells expressing split GFP1-
376 10 or GFP11 (Kindly provided by Prof. Dr. Oliver Schwarz, the Pasteur Institute, France⁵⁹) were
377 mixed 1:1 at the final density of 6x10⁵ cells/mL. Then 500 µl cells were co-transfected with 350
378 ng of ACE2 and 350 ng of Spike expressing vectors using LT1. 40 hours post-transfection,
379 fluorescence microscopy images were acquired using the Cytation 3 microplate reader (BioTek
380 Instruments) and the GFP area was quantified using Fiji ImageJ.

381 **Whole-cell and cell-free lysates.** Whole-cell lysates were prepared by collecting cells in
382 phosphate-buffered Saline (PBS, Gibco), pelleting (500 g, 4°C, 5 min), lysing (1 h, 4°C), and
383 clearing (14,000 rpm, 4°C, 10 min). Viral particles were filtered through a 0.45 µm MF-Millipore
384 Filter (Millex) and lysed in 1X Protein Sample Loading Buffer (LI-COR). All protein samples
385 with loading buffer were heated at 95°C for 10 min and stored at -20°C.

386 **SDS-PAGE and immunoblotting.** Whole-cell lysates were separated on NuPAGE 4- 12% Bis-
387 Tris Gels (Invitrogen) for 90 min at 120 V and blotted at constant 30 V for 30 min onto 0.45 µm
388 Immobilon-FL PVDF membrane (Merck Millipore). After the transfer, the membrane was blocked
389 in 1% casein in PBS (Thermo Scientific) and stained using primary antibodies directed against
390 strep (1:5,000, Thermo Fisher Scientific, PA5-119611), V5-tag (1:1,000, Cell Signalling, #13202),
391 VSV-M (1:2,000, Absolute Antibody, 23H12, #Ab01404-2.0), or GAPDH (1:1,000, BioLegend,
392 #631401). Infrared Dye labeled secondary antibodies IRDye 800CW Goat anti-Mouse #926-
393 32210, IRDye 800CW Goat anti-Rat (#926-32219), IRDye 680CW Goat anti-Rabbit (#925-
394 68071), IRDye 680CW Goat anti-Mouse (#926-68070), IRDye 800CW Goat anti-Rabbit (#926-
395 32211) were used, all 1:10,000. Proteins were detected using a LI-COR Odyssey scanner.

396 **Sera from vaccinated individuals.** Blood samples of ChAdOx1-nCoV-19/ BNT162b2/
397 BNT162b2 and BNT162b2/ BNT162b2/ BNT162b2 vaccinated non-coalescent individuals were
398 obtained after the participants information and written consent. Samples were collected 11-15 days
399 after the third dose using S-Monovette Serum Gel tubes (Sarstedt). Before use, the serum was heat-
400 treated at (56 °C, 30 min). Ethics approval was given by the Ethic Committee of Ulm University
401 (vote 99/21– FSt/Sta).

402 **Sequence logo and alignments.** Alignments of coronavirus and ACE2 sequences were performed
403 using ClustalW⁶⁰ with a gapOpening penalty of 80. Sequence logos were generated using R
404 packages ggplot2 and ggseqlogo⁶¹.

405 **Molecular dynamics simulation.** Molecular dynamics simulations were used to investigate the
406 interaction between the SARS-CoV-2 spike and ACE2. For this purpose, the protein structure from
407 the Protein Data Bank60 (PDB) with the ID code 3KBH was used. Atomic positions were taken
408 and then equilibrated using ReaxFF61 simulations within the Amsterdam Modeling Suite 2021
409 (<http://www.scm.com>) for 0.5 ns at 300 K. Subsequently, the amino acids in position 354 were
410 replaced and the system was equilibrated again for 0.5 ns at 300 K using ReaxFF simulations.
411 Then, the interaction energy was calculated by running ReaxFF simulations in the NVT ensemble
412 for 25 ps while the system was coupled to a Berendsen heat bath with a temperature of 300 K and
413 a coupling constant of 100 fs.

414 **Statistics.** Statistical analyses were performed using GraphPad Prism 9.4.1 (GraphPad Software).
415 P-values were determined using a two-tailed Student's t-test with Welch's correction. Unless
416 otherwise stated, data are shown as the mean of at least three independent experiments \pm SEM.

417 **Acknowledgments**

418 We thank Regina Burger and Daniela Krnavek for technical assistance. The ACE2 vector and the
419 SARS-CoV-2 S-HA plasmid were kindly provided by Shinji Makino and Stefan Pöhlmann. C.P.,
420 A.S. and S.N. are part of the International Graduate school for Molecular Medicine (IGradU), Ulm.
421 This study was supported by DFG grants to F.K. (CRC 1279), T.J. (CRC 1279) and K.M.J.S.
422 (CRC1279). F.K. and K.M.J.S. were supported by the BMBF (Restrict SARS-CoV-2 and
423 IMMUNOMOD). J.A.M. received funding from the DFG (MU 4485/1-1).

424 **Author Contributions**

425 Q.W. performed most experiments. S.N., Q.X., C.P. and F.Z. supported Q.W. and performed
426 cell-to-cell fusion and neutralization assays. C.J. and T.J. performed molecular modeling analyses.
427 A.S. and J.A.M. provided serum samples. Q.W. F.Z., K.M.J.S. and F.K. conceived the study,
428 planned experiments and wrote the manuscript. All authors reviewed and approved the manuscript.

429 **Competing interests**

430 The authors declare no competing interests.

431 **References**

- 432 1. Mahdy, M.A.A., Younis, W., and Ewaida, Z. (2020). An Overview of SARS-CoV-2 and
433 Animal Infection. *Frontiers in Veterinary Science* 7.
- 434 2. Dhama, K., Patel, S.K., Sharun, K., Pathak, M., Tiwari, R., Yatoo, M.I., Malik, Y.S., Sah, R.,
435 Rabaan, A.A., Panwar, P.K., et al. (2020). SARS-CoV-2 jumping the species barrier: Zoonotic
436 lessons from SARS, MERS and recent advances to combat this pandemic virus. *Travel Med
437 Infect Dis* 37, 101830. 10.1016/j.tmaid.2020.101830.
- 438 3. Banerjee, A., Kulcsar, K., Misra, V., Frieman, M., and Mossman, K. (2019). Bats and
439 Coronaviruses. *Viruses* 11. 10.3390/v11010041.
- 440 4. Ye, Z.W., Yuan, S., Yuen, K.S., Fung, S.Y., Chan, C.P., and Jin, D.Y. (2020). Zoonotic origins
441 of human coronaviruses (NLM (Medline)) 10.7150/ijbs.45472.
- 442 5. Corman, V.M., Muth, D., Niemeyer, D., and Drosten, C. (2018). Hosts and Sources of
443 Endemic Human Coronaviruses. In *Advances in Virus Research* (Academic Press Inc.), pp.
444 163–188. 10.1016/bs.aivir.2018.01.001.
- 445 6. Cui, J., Li, F., and Shi, Z.L. (2019). Origin and evolution of pathogenic coronaviruses (Nature
446 Publishing Group) 10.1038/s41579-018-0118-9.
- 447 7. Brüssow, H., and Brüssow, L. (2021). Clinical evidence that the pandemic from 1889 to 1891
448 commonly called the Russian flu might have been an earlier coronavirus pandemic. *Microbial
449 Biotechnology* 14, 1860–1870. 10.1111/1751-7915.13889.
- 450 8. Ksiazek, T.G., Erdman, D., Goldsmith, C.S., Zaki, S.R., Peret, T., Emery, S., Tong, S., Urbani,
451 C., Comer, J.A., Lim, W., et al. (2003). A novel coronavirus associated with severe acute
452 respiratory syndrome. *New England Journal of Medicine* 348, 1953–1966.
453 10.1056/NEJMoa030781.
- 454 9. Bermingham, A., Chand, M.A., Brown, C.S., Aarons, E., Tong, C., Langrish, C., Hoschler,
455 K., Brown, K., Galiano, M., Myers, R., et al. (2012). Severe respiratory illness caused by a
456 novel coronavirus, in a patient transferred to the United Kingdom from the Middle East,
457 September 2012. *Eurosurveillance* 17. 10.2807/ese.17.40.20290-en.
- 458 10. Zhou, P., Yang, X.L., Wang, X.G., Hu, B., Zhang, L., Zhang, W., Si, H.R., Zhu, Y., Li, B.,
459 Huang, C.L., et al. (2020). A pneumonia outbreak associated with a new coronavirus of
460 probable bat origin. *Nature* 579, 270–273. 10.1038/s41586-020-2012-7.
- 461 11. Lu, R., Zhao, X., Li, J., Niu, P., Yang, B., Wu, H., Wang, W., Song, H., Huang, B., Zhu, N.,
462 et al. (2020). Genomic characterisation and epidemiology of 2019 novel coronavirus:
463 implications for virus origins and receptor binding. *Lancet* 395, 565–574. 10.1016/S0140-
464 6736(20)30251-8.

465 12. Boni, M.F., Lemey, P., Jiang, X., Lam, T.T.Y., Perry, B.W., Castoe, T.A., Rambaut, A., and
466 Robertson, D.L. (2020). Evolutionary origins of the SARS-CoV-2 sarbecovirus lineage
467 responsible for the COVID-19 pandemic. *Nature Microbiology*, 1–10. 10.1038/s41564-020-
468 0771-4.

469 13. Ge, X.-Y., Li, J.-L., Yang, X.-L., Chmura, A.A., Zhu, G., Epstein, J.H., Mazet, J.K., Hu, B.,
470 Zhang, W., Peng, C., et al. (2013). Isolation and characterization of a bat SARS-like
471 coronavirus that uses the ACE2 receptor. *Nature* 503, 535–538. 10.1038/nature12711.

472 14. Li, W., Shi, Z., Yu, M., Ren, W., Smith, C., Epstein, J.H., Wang, H., Crameri, G., Hu, Z.,
473 Zhang, H., et al. (2005). Bats Are Natural Reservoirs of SARS-Like Coronaviruses. *Science*
474 310, 676–679. 10.1126/science.1118391.

475 15. Lam, T.T.Y., Shum, M.H.H., Zhu, H.C., Tong, Y.G., Ni, X.B., Liao, Y.S., Wei, W., Cheung,
476 W.Y.M., Li, W.J., Li, L.F., et al. (2020). Identifying SARS-CoV-2 related coronaviruses in
477 Malayan pangolins. *Nature*. 10.1038/s41586-020-2169-0.

478 16. Wacharapluesadee, S., Tan, C.W., Maneeorn, P., Duengkae, P., Zhu, F., Joyjinda, Y.,
479 Kaewpom, T., Chia, W.N., Ampoot, W., Lim, B.L., et al. (2021). Evidence for SARS-CoV-2
480 related coronaviruses circulating in bats and pangolins in Southeast Asia. *Nat Commun* 12,
481 972. 10.1038/s41467-021-21240-1.

482 17. Guan, Y., Zheng, B.J., He, Y.Q., Liu, X.L., Zhuang, Z.X., Cheung, C.L., Luo, S.W., Li, P.H.,
483 Zhang, L.J., Guan, Y.J., et al. (2003). Isolation and characterization of viruses related to the
484 SARS coronavirus from animals in southern China. *Science* 302, 276–278.
485 10.1126/science.1087139.

486 18. Hoffmann, M., Kleine-Weber, H., Schroeder, S., Krüger, N., Herrler, T., Erichsen, S.,
487 Schiergens, T.S., Herrler, G., Wu, N.-H., Nitsche, A., et al. (2020). SARS-CoV-2 Cell Entry
488 Depends on ACE2 and TMPRSS2 and Is Blocked by a Clinically Proven Protease Inhibitor.
489 *Cell*. 10.1016/j.cell.2020.02.052.

490 19. Hofmann, H., Pyrc, K., van der Hoek, L., Geier, M., Berkhout, B., and Pöhlmann, S. (2005).
491 Human coronavirus NL63 employs the severe acute respiratory syndrome coronavirus
492 receptor for cellular entry. *Proc Natl Acad Sci U S A* 102, 7988–7993.
493 10.1073/pnas.0409465102.

494 20. Letko, M., Marzi, A., and Munster, V. (2020). Functional assessment of cell entry and receptor
495 usage for SARS-CoV-2 and other lineage B betacoronaviruses. *Nature Microbiology* 5, 562–
496 569. 10.1038/s41564-020-0688-y.

497 21. Zhou, H., Ji, J., Chen, X., Bi, Y., Li, J., Wang, Q., Hu, T., Song, H., Zhao, R., Chen, Y., et al.
498 (2021). Identification of novel bat coronaviruses sheds light on the evolutionary origins of
499 SARS-CoV-2 and related viruses. *Cell* 184, 4380-4391.e14. 10.1016/j.cell.2021.06.008.

500 22. Zhou, H., Chen, X., Hu, T., Li, J., Song, H., Liu, Y., Wang, P., Liu, D., Yang, J., Holmes, E.C.,
501 et al. (2020). A Novel Bat Coronavirus Closely Related to SARS-CoV-2 Contains Natural
502 Insertions at the S1/S2 Cleavage Site of the Spike Protein. *Curr Biol* 30, 2196-2203.e3.
503 10.1016/j.cub.2020.05.023.

504 23. Evans, T.S., Tan, C.W., Aung, O., Phyu, S., Lin, H., Coffey, L.L., Toe, A.T., Aung, P., Aung, T.H., Aung, N.T., et al. (2023). Exposure to diverse sarbecoviruses indicates frequent zoonotic spillover in human communities interacting with wildlife. *Int J Infect Dis*, S1201-9712(23)00064-4. 10.1016/j.ijid.2023.02.015.

508 24. Starr, T.N., Zepeda, S.K., Walls, A.C., Greaney, A.J., Alkhovsky, S., Veesler, D., and Bloom, J.D. (2022). ACE2 binding is an ancestral and evolvable trait of sarbecoviruses. *Nature* 603, 913–918. 10.1038/s41586-022-04464-z.

511 25. Lin, H.-X., Feng, Y., Wong, G., Wang, L., Li, B., Zhao, X., Li, Y., Smaill, F., and Zhang, C. (2008). Identification of residues in the receptor-binding domain (RBD) of the spike protein of human coronavirus NL63 that are critical for the RBD-ACE2 receptor interaction. *J Gen Virol* 89, 1015–1024. 10.1099/vir.0.83331-0.

515 26. Zech, F., Schniertshauer, D., Jung, C., Herrmann, A., Cordsmeier, A., Xie, Q., Nchioua, R., Prelli Bozzo, C., Volcic, M., Koepke, L., et al. (2021). Spike residue 403 affects binding of coronavirus spikes to human ACE2. *Nat Commun* 12, 6855. 10.1038/s41467-021-27180-0.

518 27. Golcuk, M., Yildiz, A., and Gur, M. (2021). The Omicron Variant Increases the Interactions of SARS-CoV-2 Spike Glycoprotein with ACE2 10.1101/2021.12.06.471377.

520 28. Liu, K., Pan, X., Li, L., Yu, F., Zheng, A., Du, P., Han, P., Meng, Y., Zhang, Y., Wu, L., et al. (2021). Binding and molecular basis of the bat coronavirus RaTG13 virus to ACE-2 in humans and other species. *Cell*. 10.1016/j.cell.2021.05.031.

523 29. Wrobel, A.G., Benton, D.J., Xu, P., Roustan, C., Martin, S.R., Rosenthal, P.B., Skehel, J.J., and Gamblin, S.J. (2020). SARS-CoV-2 and bat RaTG13 spike glycoprotein structures inform on virus evolution and furin-cleavage effects. *Nat Struct Mol Biol* 27, 763–767. 10.1038/s41594-020-0468-7.

527 30. Xiao, K., Zhai, J., Feng, Y., Zhou, N., Zhang, X., Zou, J.-J., Li, N., Guo, Y., Li, X., Shen, X., et al. (2020). Isolation of SARS-CoV-2-related coronavirus from Malayan pangolins. *Nature*. 10.1038/s41586-020-2313-x.

530 31. Haagmans, B.L., Al Dhahiry, S.H.S., Reusken, C.B.E.M., Raj, V.S., Galiano, M., Myers, R., Godeke, G.-J., Jonges, M., Farag, E., Diab, A., et al. (2014). Middle East respiratory syndrome coronavirus in dromedary camels: an outbreak investigation. *Lancet Infect Dis* 14, 140–145. 10.1016/S1473-3099(13)70690-X.

534 32. Jackson, C.B., Farzan, M., Chen, B., and Choe, H. (2022). Mechanisms of SARS-CoV-2 entry into cells. *Nat Rev Mol Cell Biol* 23, 3–20. 10.1038/s41580-021-00418-x.

536 33. Cheng, Y.-R., Li, X., Zhao, X., and Lin, H. (2021). Cell Entry of Animal Coronaviruses. *Viruses* 13, 1977. 10.3390/v13101977.

538 34. Oude Munnink, B.B., Sikkema, R.S., Nieuwenhuijse, D.F., Molenaar, R.J., Munger, E., Molenkamp, R., van der Spek, A., Tolsma, P., Rietveld, A., Brouwer, M., et al. (2021). Transmission of SARS-CoV-2 on mink farms between humans and mink and back to humans. *Science* 371, 172–177. 10.1126/science.abe5901.

542 35. Frazzini, S., Amadori, M., Turin, L., and Riva, F. (2022). SARS CoV-2 infections in animals,
543 two years into the pandemic. *Arch Virol* 167, 2503–2517. 10.1007/s00705-022-05609-1.

544 36. Islam, A., Ferdous, J., Islam, S., Sayeed, M.A., Rahman, M.K., Saha, O., Hassan, M.M., and
545 Shirin, T. (2022). Transmission dynamics and susceptibility patterns of SARS-CoV-2 in
546 domestic, farmed and wild animals: Sustainable One Health surveillance for conservation and
547 public health to prevent future epidemics and pandemics. *Transbound Emerg Dis* 69, 2523–
548 2543. 10.1111/tbed.14356.

549 37. Pastorio, C., Zech, F., Noettger, S., Jung, C., Jacob, T., Sanderson, T., Sparrer, K.M.J., and
550 Kirchhoff, F. (2022). Determinants of Spike infectivity, processing, and neutralization in
551 SARS-CoV-2 Omicron subvariants BA.1 and BA.2. *Cell Host & Microbe* 30, 1255-1268.e5.
552 10.1016/j.chom.2022.07.006.

553 38. Kimura, I., Yamasoba, D., Tamura, T., Nao, N., Suzuki, T., Oda, Y., Mitoma, S., Ito, J.,
554 Nasser, H., Zahradnik, J., et al. (2022). Virological characteristics of the SARS-CoV-2
555 Omicron BA.2 subvariants, including BA.4 and BA.5. *Cell* 185, 3992-4007.e16.
556 10.1016/j.cell.2022.09.018.

557 39. Tegally, H., Moir, M., Everatt, J., Giovanetti, M., Scheepers, C., Wilkinson, E., Subramoney,
558 K., Makatini, Z., Moyo, S., Amoako, D.G., et al. (2022). Emergence of SARS-CoV-2 Omicron
559 lineages BA.4 and BA.5 in South Africa. *Nat Med* 28, 1785–1790. 10.1038/s41591-022-
560 01911-2.

561 40. Wang, Q., Guo, Y., Iketani, S., Nair, M.S., Li, Z., Mohri, H., Wang, M., Yu, J., Bowen, A.D.,
562 Chang, J.Y., et al. (2022). Antibody evasion by SARS-CoV-2 Omicron subvariants BA.2.12.1,
563 BA.4 and BA.5. *Nature* 608, 603–608. 10.1038/s41586-022-05053-w.

564 41. Marra, M.A., Jones, S.J.M., Astell, C.R., Holt, R.A., Brooks-Wilson, A., Butterfield, Y.S.N.,
565 Khattra, J., Asano, J.K., Barber, S.A., Chan, S.Y., et al. (2003). The Genome sequence of the
566 SARS-associated coronavirus. *Science* 300, 1399–1404. 10.1126/science.1085953.

567 42. Wang, M., Yan, M., Xu, H., Liang, W., Kan, B., Zheng, B., Chen, H., Zheng, H., Xu, Y.,
568 Zhang, E., et al. (2005). SARS-CoV infection in a restaurant from palm civet. *Emerg Infect
569 Dis* 11, 1860–1865. 10.3201/eid1112.041293.

570 43. Tao, Y., and Tong, S. (2019). Complete Genome Sequence of a Severe Acute Respiratory
571 Syndrome-Related Coronavirus from Kenyan Bats. *Microbiol Resour Announc* 8, e00548-19.
572 10.1128/MRA.00548-19.

573 44. Drexler, J.F., Gloza-Rausch, F., Glende, J., Corman, V.M., Muth, D., Goettsche, M., Seebens,
574 A., Niedrig, M., Pfefferle, S., Yordanov, S., et al. (2010). Genomic characterization of severe
575 acute respiratory syndrome-related coronavirus in European bats and classification of
576 coronaviruses based on partial RNA-dependent RNA polymerase gene sequences. *J Virol* 84,
577 11336–11349. 10.1128/JVI.00650-10.

578 45. Wu, K., Li, W., Peng, G., and Li, F. (2009). Crystal structure of NL63 respiratory coronavirus
579 receptor-binding domain complexed with its human receptor. *Proc Natl Acad Sci U S A* 106,
580 19970–19974. 10.1073/pnas.0908837106.

581 46. Seidel, A., Zanoni, M., Groß, R., Krnavek, D., Erdemci-Evin, S., von Maltitz, P., Albers, D.P.J., Conzelmann, C., Liu, S., Weil, T., et al. (2022). BNT162b2 booster after heterologous
582 prime-boost vaccination induces potent neutralizing antibodies and T cell reactivity against
583 SARS-CoV-2 Omicron BA.1 in young adults. *Front Immunol* 13, 882918. 10.3389/fimmu.2022.882918.

586 47. Groß, R., Zanoni, M., Seidel, A., Conzelmann, C., Gilg, A., Krnavek, D., Erdemci-Evin, S.,
587 Mayer, B., Hoffmann, M., Pöhlmann, S., et al. (2021). Heterologous ChAdOx1 nCoV-19 and
588 BNT162b2 prime-boost vaccination elicits potent neutralizing antibody responses and T cell
589 reactivity against prevalent SARS-CoV-2 variants. *EBioMedicine* 75, 103761. 10.1016/j.ebiom.2021.103761.

591 48. Cantoni, D., Mayora-Neto, M., Thakur, N., Elrefaei, A.M.E., Newman, J., Vishwanath, S.,
592 Nadesalingam, A., Chan, A., Smith, P., Castillo-Olivares, J., et al. (2022). Pseudotyped Bat
593 Coronavirus RaTG13 is efficiently neutralised by convalescent sera from SARS-CoV-2
594 infected patients. *Commun Biol* 5, 409. 10.1038/s42003-022-03325-9.

595 49. Uraki, R., Halfmann, P.J., Iida, S., Yamayoshi, S., Furusawa, Y., Kiso, M., Ito, M., Iwatsuki-
596 Horimoto, K., Mine, S., Kuroda, M., et al. (2022). Characterization of SARS-CoV-2 Omicron
597 BA.4 and BA.5 isolates in rodents. *Nature* 612, 540–545. 10.1038/s41586-022-05482-7.

598 50. Wong, A.C.P., Li, X., Lau, S.K.P., and Woo, P.C.Y. (2019). Global Epidemiology of Bat
599 Coronaviruses. *Viruses* 11, 174. 10.3390/v11020174.

600 51. Murakami, S., Kitamura, T., Suzuki, J., Sato, R., Aoi, T., Fujii, M., Matsugo, H., Kamiki, H.,
601 Ishida, H., Takenaka-Uema, A., et al. (2020). Detection and Characterization of Bat
602 Sarbecovirus Phylogenetically Related to SARS-CoV-2, Japan. *Emerg Infect Dis* 26, 3025–
603 3029. 10.3201/eid2612.203386.

604 52. Crook, J.M., Murphy, I., Carter, D.P., Pullan, S.T., Carroll, M., Vipond, R., Cunningham,
605 A.A., and Bell, D. (2021). Metagenomic identification of a new sarbecovirus from horseshoe
606 bats in Europe. *Sci Rep* 11, 14723. 10.1038/s41598-021-94011-z.

607 53. Hu, B., Ge, X., Wang, L.-F., and Shi, Z. (2015). Bat origin of human coronaviruses. *Virol J*
608 12, 221. 10.1186/s12985-015-0422-1.

609 54. Van Der Hoek, L., Pyrc, K., Jebbink, M.F., Vermeulen-Oost, W., Berkhout, R.J.M., Wolthers,
610 K.C., Wertheim-Van Dillen, P.M.E., Kaandorp, J., Spaargaren, J., and Berkhout, B. (2004).
611 Identification of a new human coronavirus. *Nature Medicine* 10, 368–373. 10.1038/nm1024.

612 55. Dangi, T., Palacio, N., Sanchez, S., Park, M., Class, J., Visvabharathy, L., Ciucci, T., Koralnik,
613 I.J., Richner, J.M., and Penaloza-MacMaster, P. (2021). Cross-protective immunity following
614 coronavirus vaccination and coronavirus infection. *J Clin Invest*. 10.1172/JCI151969.

615 56. Lawrenz, J., Xie, Q., Zech, F., Weil, T., Seidel, A., Krnavek, D., van der Hoek, L., Münch, J.,
616 Müller, J.A., and Kirchhoff, F. (2022). Severe Acute Respiratory Syndrome Coronavirus 2
617 Vaccination Boosts Neutralizing Activity Against Seasonal Human Coronaviruses. *Clinical
618 Infectious Diseases* 75, e653–e661. 10.1093/cid/ciac057.

619 57. Saville, J.W., Mannar, D., Zhu, X., Berezuk, A.M., Cholak, S., Tuttle, K.S., VahdatiHassani,
620 F., and Subramaniam, S. (2023). Structural analysis of receptor engagement and antigenic drift
621 within the BA.2 spike protein. *Cell Rep* 42, 111964. 10.1016/j.celrep.2022.111964.

622 58. Tang, L., Zhang, D., Han, P., Kang, X., Zheng, A., Xu, Z., Zhao, X., Wang, V.Y.-F., Qi, J.,
623 Wang, Q., et al. (2022). Structural basis of SARS-CoV-2 and its variants binding to
624 intermediate horseshoe bat ACE2. *Int J Biol Sci* 18, 4658–4668. 10.7150/ijbs.73640.

625 59. Buchrieser, J., Dufloo, J., Hubert, M., Monel, B., Planas, D., Rajah, M.M., Planchais, C.,
626 Porrot, F., Guivel-Benhassine, F., Van der Werf, S., et al. (2020). Syncytia formation by
627 SARS-CoV-2-infected cells. *EMBO J* 39, e106267. 10.15252/embj.2020106267.

628 60. Larkin, M.A., Blackshields, G., Brown, N.P., Chenna, R., McGettigan, P.A., McWilliam, H.,
629 Valentin, F., Wallace, I.M., Wilm, A., Lopez, R., et al. (2007). Clustal W and Clustal X version
630 2.0. *Bioinformatics* 23, 2947–2948. 10.1093/bioinformatics/btm404.

631 61. Wagih, O. (2017). ggseqlogo: a versatile R package for drawing sequence logos.
632 *Bioinformatics* 33, 3645–3647. 10.1093/bioinformatics/btx469.

633

634 **FIGURE LEGENDS**

635 **Figure 1 | Potential origin of human CoVs and phylogenetic relationship of Spike and ACE2**
636 **proteins analyzed.** **a**, Schematic representation of the potential cross-species transmissions that
637 led to the emergence of the seven human CoVs. Highly pathogenic CoVs are indicated in red and
638 circulating CoVs in blue. Those utilizing ACE2 are underlined. In some cases, the intermediate
639 hosts are unknown or under debate. Images were derived from Biorender. **b-c**, Phylogenetic
640 relationship between the Spike (b) and ACE2 (c) amino acid sequences from the indicated viral
641 strains or species, respectively.

642 **Figure 2 | Utilization of ACE2 receptors from different species by SARS-CoV-2 variants.** **a**,
643 Automatic quantification of infection events of HEK293T cells expressing the various ACE2
644 receptors and transduced with VSVΔG-GFP pseudotyped with the indicated SARS-CoV-2 S
645 proteins or lacking S (CTRL). Bars in all panels represent the mean of three experiments (\pm SEM).
646 Statistical significance was determined by unpaired t tested; *p < 0.05; **p < 0.01; ***p < 0.001.
647 Background was generally increased for BA.5 S, possibly due to low levels of ACE2 independent
648 infection of the target cells. **b**, Immunoblot of whole cells lysates of HEK293T cells expressing
649 BA.2, BA.4/5 or the indicated mutant S proteins. Blots were stained with anti-V5 tag and anti-
650 GAPDH. **c**, Infection of HEK293T cells transfected with an empty control vector (grey) of the *Rf*
651 (yellow), *Ra* (orange) or human (red) ACE2 receptors. Numbers above bars indicate n-fold
652 enhancement compared to control. **d**, Schematic diagram of wild-type and R493Q BA.2 S with
653 the *Rf* ACE2. Potential van der Waals interactions and hydrogen bonds of BA.2 spike R493 with
654 *Rf* ACE2 D31 and E35 are indicated by dash back lines and pink lines, respectively. **e**, Ability of
655 wild-type and mutant *Rf* ACE2 receptors for BA.5 S-mediated infection of VSVpp. If not indicated
656 otherwise, p-values indicate difference to the wild-type *Rf* ACE2 receptor. Human and *Ra* ACE2
657 are shown for control.

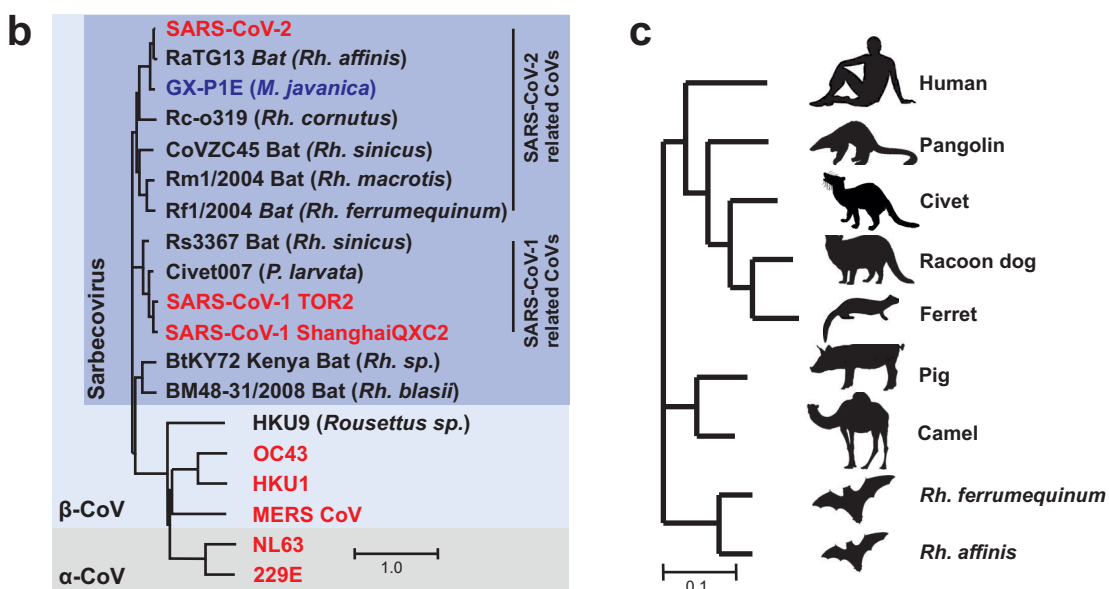
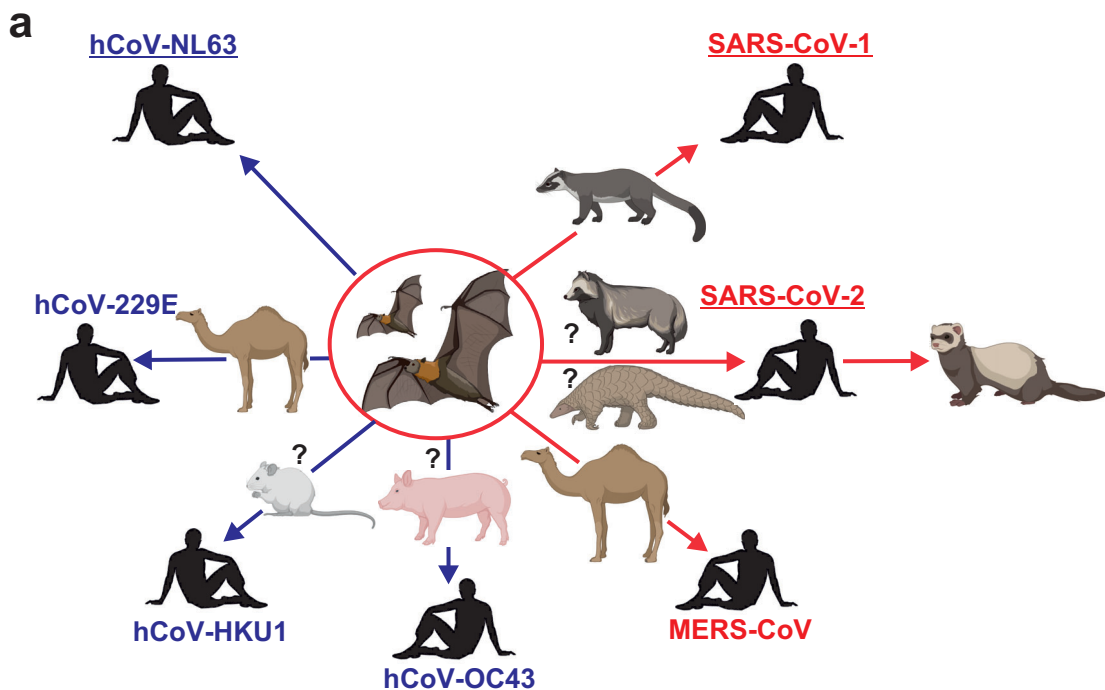
658 **Figure 3 | Species-specific utilization of ACE2 by S-proteins of bat, pangolin and civet CoVs.**

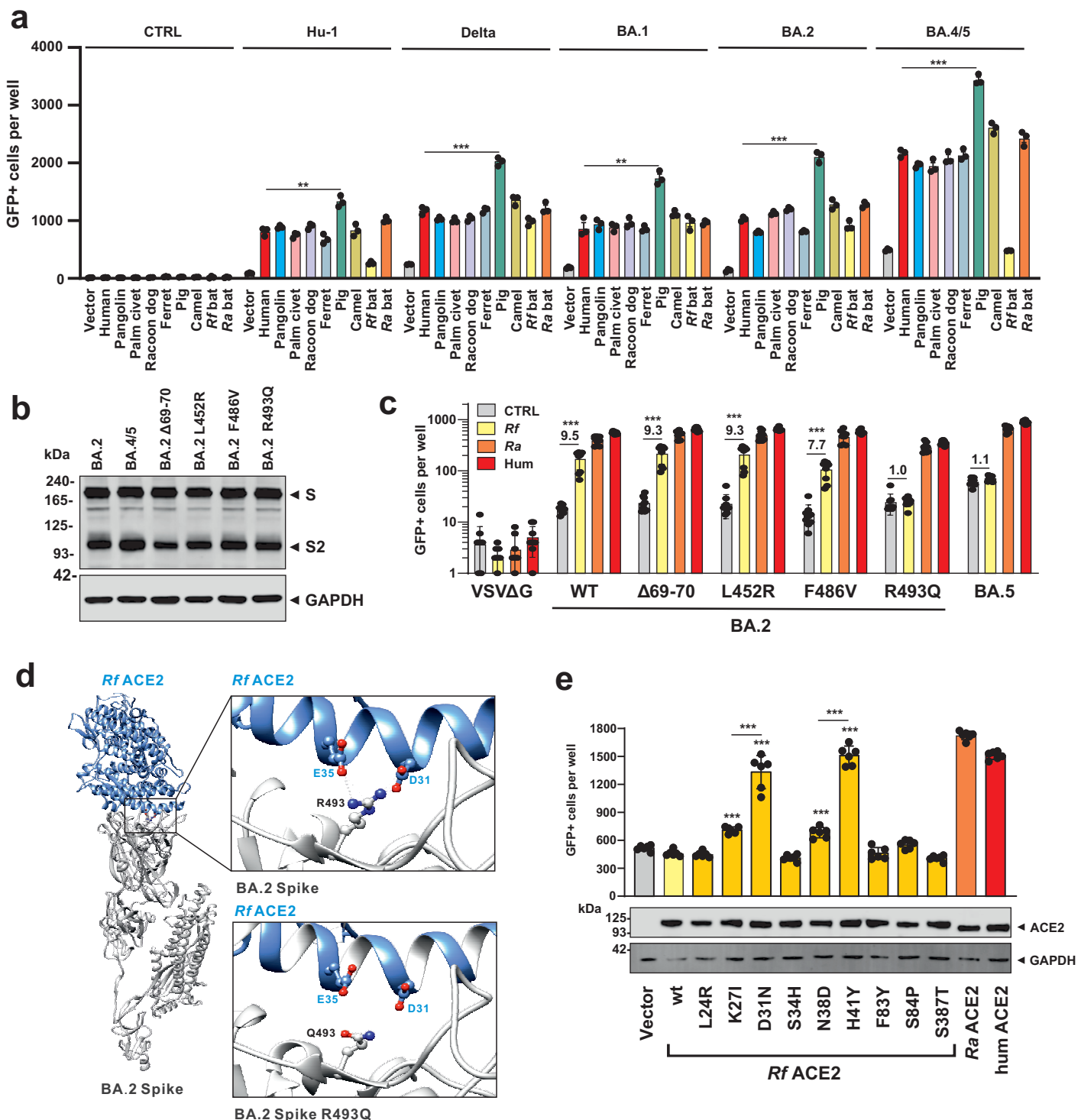
659 **a**, Automatic quantification of infection events of HEK293T cells expressing the indicated ACE2
660 receptors infected by VSVpp carrying S proteins of SARS-CoVs or animal CoVs. Bars represent
661 the mean of three experiments (\pm SEM). Statistical significance was tested by unpaired t test; **p
662 < 0.01 . **b**, Infection kinetics of ACE2 expressing HEK293T cells infected by VSVpp containing
663 the indicated mutant S proteins. Infected GFP+ cells were automatically quantified over a period
664 of 24 h.

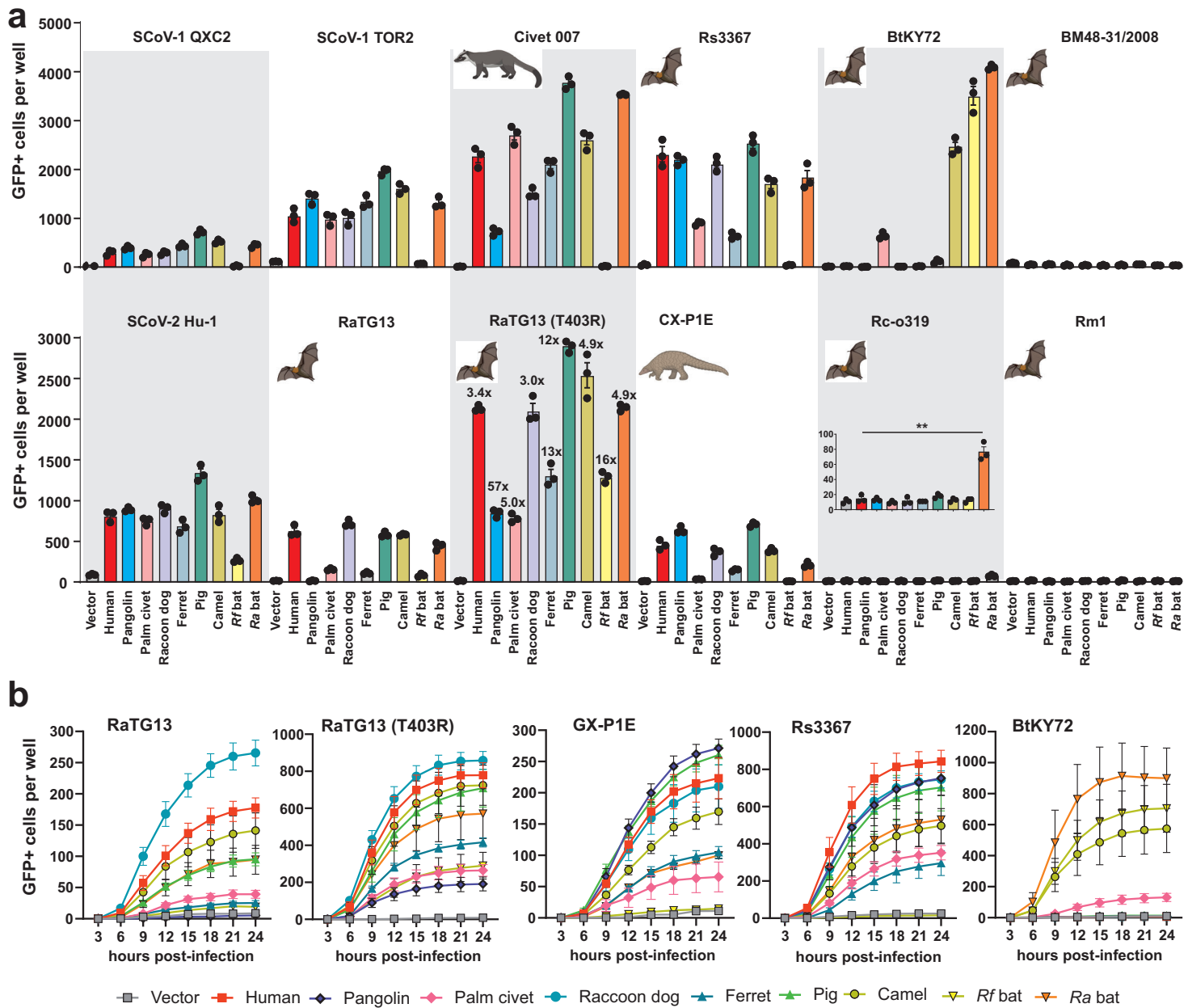
665 **Figure 4 | Species-specificity of ACE2 receptor usage by hCoV-NL63.** **a**, Infection of HEK293T
666 cells expressing the indicated ACE2 receptors by VSVpp carrying S proteins of MERS-CoV or
667 circulating hCoVs. Bars represent the mean of three experiments (\pm SEM). **b**, Alignment of the
668 amino acids in the corresponding region of ACE2 receptors used for functional analyses. **c**,
669 Position of the G354H variation in ACE2 at the interaction site with the RBD of the hCoV-NL63
670 S protein. **d**, Exemplary energy curve of the reactive molecular dynamics simulation for hCoV-
671 NL63 S with human, ferret and pangolin ACE2 receptors.

672 **Figure 5 | Neutralization of S proteins from human and bat CoVs.** **a**, Neutralization of VSVpp
673 carrying the S proteins of the indicated human and bat CoVs by sera obtained from five
674 AZ/BNT/BNT (upper) or five 3xBNT (lower) vaccinated individuals compared to the untreated
675 control (set to 100%). Shown are mean values obtained for the five sera, each tested in ten technical
676 replicates. Infection was measured in HEK293T cells expressing human or bat (right panel) ACE2.
677 **b**, TCID₅₀ values obtained for neutralization of the indicated S proteins by individual sera as
678 described under panel a. Symbols indicate individual donors and orange lines the average value
679 obtained for the five sera from the respective groups. **c**, Correlation between the IC₅₀ values
680 obtained for the AZ/2xBt and 3xBt groups. Human S proteins are indicated by red and bat S
681 proteins by black symbols. Percentages indicate amino acid identity to the SARS-CoV-2 S protein.

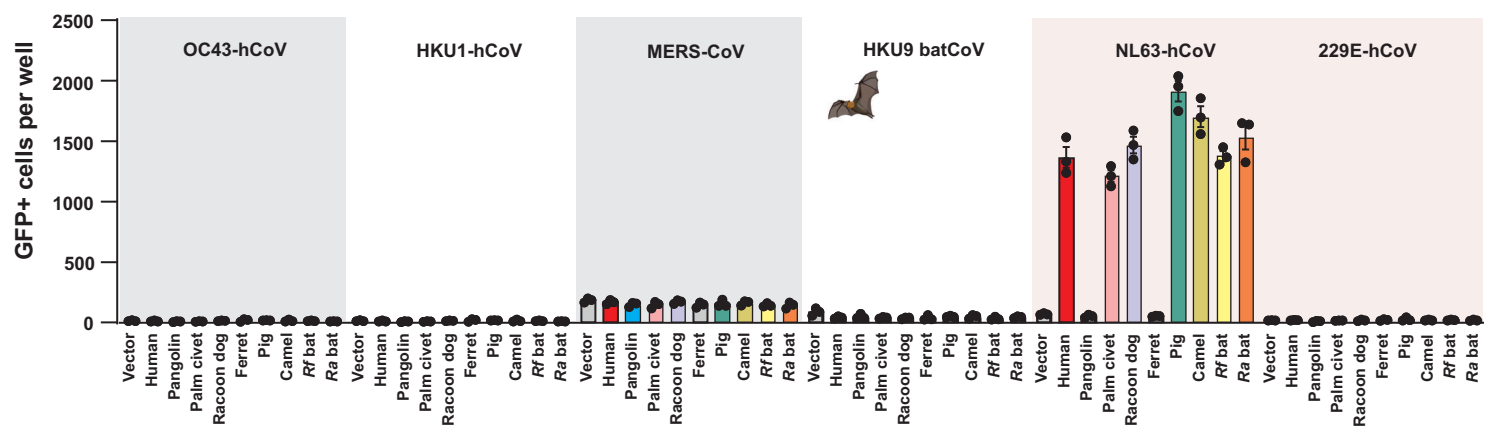
682 **Figure 6 | Overview on ACE2 usage by CoV S proteins and possible cross-species**
683 **transmissions.** **a**, Binned heatmap of the infection efficiency of various ACE2-S combination.
684 Data aggregated from Figure 2a, 3a and 4a. **b**, Chord diagram of the data in (a) depicting the
685 efficiency of indicated S-ACE2 mediated infection as scaled connectors. Left panel: SARS-CoV-
686 2 Hu-1 (blue) and Variants of concern (Delta, red; Omicron, purple). Right panel: assorted SARS-
687 CoV-2-related CoVs (blue and purple) and SARS-CoV-1-related CoVs (red) compared to bat
688 CoVs (grey). Species of ACE2 as indicated in the lower half of the panel.



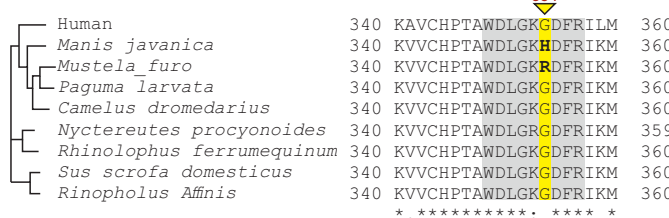




a

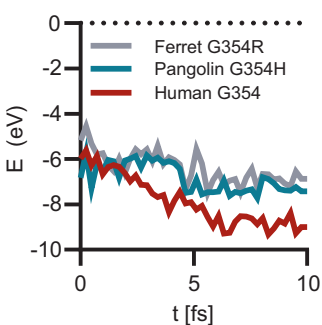
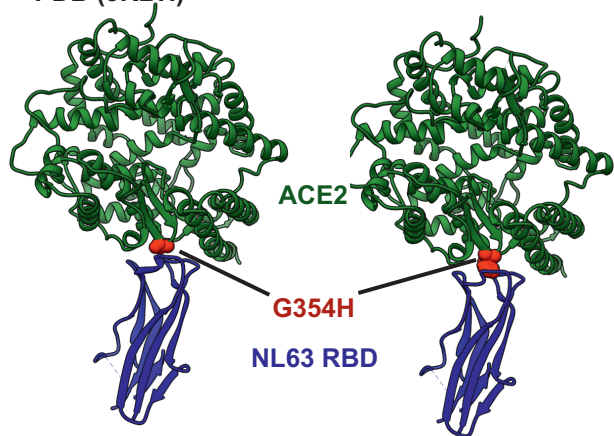


b

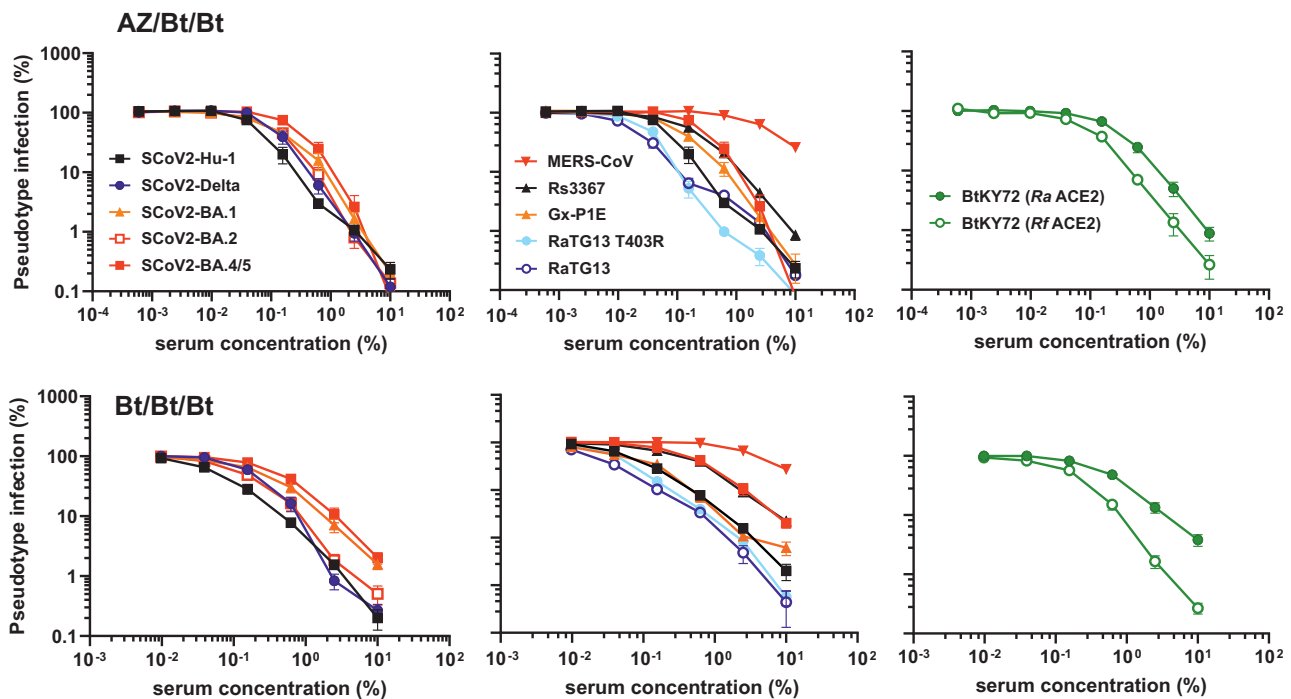


c

human: PDB (3KBH) *Manis javanica*



a



b

